form **17** is much less stable, as well as the unfavorable N-protonation would result in an unstable structure. The choice is then between the C-protonated structures **14** and **15.** The relative heats of formation would indicate that **15** is more stable. This is somewhat in contradiction with the concept of protonation of **7** in the middle,[2b] as well as with our findings on the structure of the protonated dihydropyridine formed upon the reduction of 2-PAM.[3a,b] However, analyzing the possibilities of the formation of the more stable form **15,** it can be seen that it can be formed primarily from the protonation of less stable 2,3-dihydropyridine (**8**), by protonation on the N. The formation of **15** from the classical 1,2-dihydropyridine structure **7** is unfavorable from the point of view of the relative charge distribution. It seems, thus, that the protonation of 1,2-dihydropyridine (**7**) would result in the kinetically more favorable **14,** which, however, would equilibrate under appropriate conditions to the thermodynamically more stable **15.**

In conclusion, the detailed MINDO/3 study of the reduction and related processes has accurately described the relative energies and behavior of the various dihydro isomers. It can be seen that the relative energy differences among the simple isomers are not too large, and under certain conditions any of the isomers could form. The bicyclo structures **6, 10, 13,** and **17,** although not clearly dihydropyridines, are of interest and the structures certainly represent minima in the potential surface.

The energetic and conformational problems of the related biologically important dihydropyridines, such as the various N-alkyl pyridinium aldoximes[3,4] are currently being studied and the results will be published elsewhere.

References and Notes

(1) Address correspondence to this author at INTERx Research Corp., Lawrence, Kan. 66044.
(2) (a) U. Eisner and J. Kuthan, *Chem. Rev.*, **72**, 1–42 (1972); (b) R. E. Lyle and P. S. Anderson, *Adv. Heterocycl. Chem.*, **6**, 45–93 (1966).
(3) (a) N. Bodor, E. Shek, and T. Higuchi, *Science*, **190**, 155–156 (1970); (b) N. Bodor, E. Shek, and T. Higuchi, *J. Med. Chem.*, **19**, 102–108 (1976); (c) E. Shek, N. Bodor, and T. Higuchi, *ibid.*, 108–113 (1976); (d) *ibid.*, 113–117 (1976).
(4) N. Bodor, R. G. Roller, and S. H. Selk, *J. Pharm. Sci.*, in press.
(5) (a) B. Pullman and A. Pullman, *Proc. Natl. Acad. Sci. U.S.A.*, **45**, 136–144 (1959); (b) E. M. Evleth, *J. Am. Chem. Soc.*, **89**, 6445–6453 (1967); (c) J. Kuthan and L. Musil, *Collect. Czech. Chem. Commun.*, **40**, 3169–3176 (1975); (d) J. Kuthan and L. Musil, *ibid.*, **42**, 857–866 (1977).
(6) F. W. Fowler, *J. Am. Chem. Soc.*, **94**, 5926–5927 (1972).
(7) (a) R. C. Bingham, M. J. S. Dewar, and D. H. Lo, *J. Am. Chem. Soc.*, **97**, 1285–1293 (1975); (b) R. C. Bingham, M. J. S. Dewar, and D. H. Lo, *ibid.*, 1302–1306 (1975).
(8) (a) N. C. Baird and M. J. S. Dewar, *J. Am. Chem. Soc.*, **91**, 352–357 (1969); (b) M. J. S. Dewar and E. Haselbach, *ibid.*, **92**, 590–598 (1970); N. Bodor, M. J. S. Dewar, A. Harget, and E. Haselbach, *ibid.*, **92**, 3854–3859 (1970); (c) N. Bodor, M. J. S. Dewar, and D. H. Lo, *ibid.*, **94**, 5304–5310 (1972).
(9) H. Koyama, J. M. M. Robinson, and F. Laves, *Nature (London)*, **50**, 40 (1963).
(10) M. J. S. Dewar, "Hyperconjugation", Ronald Press, New York, N.Y., 1962.
(11) T. Koenig and H. Longmaid, *J. Org. Chem.*, **39**, 560–562 (1974).

Theoretical Study of Li_2H. 3. Approximate Natural Orbital Contour Diagrams and Occupation Numbers for the Formation and Dissociation of Li_2H

Walter England* and Nora H. Sabelli†

Contribution from the Chemistry Division, Argonne National Laboratory, Argonne, Illinois 60439.

Received November 28, 1977

Abstract: Approximate natural orbital contour diagrams and occupation numbers are used to analyze ab initio potential energy curves along pathways that lead to the formation and dissociation of Li_2H: $H + Li_2 \rightarrow Li_2H \rightarrow LiH + Li$. In addition to the ground state, the three lowest excited states are analyzed. The analysis revealed extensive charge transfer intermediates of the type $Li_2^+H^-$. The species $LiH^-\cdots Li^+$ was also found to be an intermediate. The natural orbital description predicts in general that charge transfer is more gradual than is expected on the basis of uncorrelated molecular orbitals. However, rather abrupt natural orbital charge transfer was also encountered.

Previous theoretical work on Li_2H has been largely concerned with determining the characteristics of the ground[1-4] and low-lying excited state[2-4] potential energy surfaces. Ab initio results[1-3] predict the existence of stable Li_2H with a C_{2v} geometry, while diatomics-in-molecules work[4] predicts a linear symmetric ground state. The discrepancy with the ab initio results is apparently due to the neglect of ionic and p-symmetry terms in the diatomic states used in ref 4.[5] Li_2H is ionic in most of its low-lying states, so it seems reasonable that ionic curves should be required in the diatomic input. The p symmetry is probably necessary to stabilize the C_{2v} geometries by enabling the Li contributions to "point" toward the incoming H atom.

A mass spectrometric identification of Li_2H has recently been reported.[6] The diatomics-in-molecules results[4] are used to establish that Li_2H has a linear symmetric geometry. However, since more accurate ab initio calculations[1,2] predict that the C_{2v} symmetry is most stable, the "experimental" geometry should be viewed as questionable. The original motivation for our own calculations[2,3] was to provide potential curves for the interpretation of ongoing molecular beam experimental work.[7] There are many interesting charge transfer processes taking place in Li_2H within energies accessible to the molecular beams. The purpose of the present work is to provide a description of these processes. Correlated wave functions are required for two reasons. First, uncorrelated molecular orbital (MO) wave functions are less accurate. Any interpretation based on them is therefore questionable. Second, the MO (single configuration) wave functions for excited states which have the same symmetry as lower states do not usually satisfy the variational principle.[8] This occurs because higher single configuration states are not orthogonal to any state which is itself an upper bound to the true ground state. Therefore the

† Visiting Scientist from the Computer Center and the Department of Chemistry, University of Illinois at Chicago Circle, Chicago, Ill. 60680.

0002-7863/78/1500-4953$01.00/0

higher states are not upper bounds to true excited states, and hence can be very difficult to calculate self-consistently. This last problem is especially severe in Li_2H for many states of interest.[2]

No unique orbital set can be associated with an approximate correlated wave function. However, given an approximate correlated wave function, approximate natural orbitals (NO's) can be computed by diagonalizing the first-order density matrix.[9] The eigenvalues of the density matrix are the occupation numbers of the NO's. Thus, the NO's are uniquely defined mathematically (for a given approximate wave function) and each is associated with a definite fraction of the total number of electrons. MO's are a special case of NO's, those having integral or zero occupation numbers. In general, NO's have nonintegral and nonnegative occupation numbers that contain the contributions from nondominant correlating configurations. Because of these characteristics we feel that NO's are the best choice for interpreting the changing valence charge distributions that occur along the different reaction pathways. Such an interpretation is the major thrust of this study; we shall, however, give some comparisons between NO's, MO's, and multiconfiguration self-consistent-field orbitals (MC orbitals). The basis sets and MO, MC, and MC-CI wave functions which are analyzed in the present work are described in detail in our previous papers.[2,3] The NO's reported here were calculated by diagonalizing the first-order density matrix associated with the MC wave function.

Static ab initio descriptions of reactions are obtained from cuts through Born-Oppenheimer energy surfaces. Such descriptions can be contrasted with dynamical results which require entire potential energy surfaces plus solutions to scattering problems. The static descriptions derive a qualitative understanding of the quantitative results that would be obtained from the entire potential surface. Neither type of calculation is trivial in terms of effort and cost. Static descriptions require significantly less work but require knowing which portions of the potential energy surface are important. Our previous papers[2,3] were concerned with establishing the important regions of the Li_2H potential surfaces. We also have unpublished results which show that geometry variations in these regions introduce no new effects. Charge transfer was found to occur in reactive cones about the C_{2v}, or broadside, approach of H to Li_2. The character of the charge transfer was found to be essentially the same within the reactive cones. This was likewise found to be the case in a more detailed ab initio study of the Li_2H ground potential energy surface by Siegbahn and Schaefer[1] and has also been deduced from experimental data and suggestions.[7,10,11] Our second paper[3] reported similar reactive cones about the collinear approach of Li to the H end of LiH. It is therefore reasonable to study the formation and dissociation of Li_2H by considering the broadside approach of H to Li_2 and the collinear dissociation of Li from LiHLi. The purpose of the present paper is to analyze our previously computed wave functions[2,3] in order to understand the essentials of charge transfer in Li_2H. As was the case in our previous work, we shall not be concerned with establishing the exact point of the charge transfer: This involves substantially larger portions of the potential surfaces than are needed for understanding the overall charge transfer. As a consequence of accumulated experience, we feel that the pathways chosen on the Li_2H potential energy surfaces provide realistic descriptions of the most important reactions possible. We shall describe these in subsequent sections.

Li_2H Formation and Dissociation

Formation of Li_2H. Charge Transfer from Li_2 and Li_2* to H. These reactions are characterized by the potential energy curves and orbital contours for the C_{2v} symmetry approach of H to Li_2 shown on Figure 1a. This geometric pathway was chosen for two reasons. First, broadside collisions are the most probable in a statistical sense. Second, ab initio potential curves predict that stable Li_2H can only be formed from H + Li_2 within "reactive cones" about the C_{2v} symmetry approach.[1-3] The interpretation is that charge transfer takes place from both Li nuclei in Li_2 to produce the stable ionic molecule $Li_2^+H^-$. Since both Li nuclei participate, the molecule is slightly more stable than LiH + Li or collinear HLiLi. The latter two cases involve only one Li nucleus in the charge transfer. (Ab initio calculations predict that collinear HLiLi is unstable relative to LiH + Li.[1,3]) Ionic C_{2v} states are consistent with experimental results for the related systems H + heavy alkali dimers[10] and Na + Na_2.[12] It is reasonable to use the C_{2v} path to characterize the charge transfer within the reaction cones since the energy is rather insensitive to 15-20° deviations about the broadside approach.[1,3] Furthermore, the minimum energy geometries of Li_2H that are predicted by the ab initio calculations[1-3] have C_{2v} symmetry for all low-lying states.

The four lowest energy ab initio potential curves will be considered. These curves provide static ab initio descriptions of the reactions

$$H(^2S) + Li_2(^1\Sigma_g^+) \rightarrow HLi_2(X^2A_1) \rightarrow LiHLi(^2\Sigma_g^+) \quad (1)$$

$$H(^2S) + Li_2(^3\Sigma_u^+) \rightarrow HLi_2(X^2B_2) \rightarrow LiHLi(^2\Sigma_u^+) \quad (2)$$

$$H(^2S) + Li_2(^3\Pi_u) \rightarrow HLi_2(A^2A_1) \rightarrow LiHLi(^2\Pi_u) \quad (3)$$

$$H(^2S) + Li_2(^1\Sigma_u^+) \rightarrow HLi_2(A^2B_2) \rightarrow LiHLi(^2\Pi_g) \quad (4)$$

along the path of Figure 1a. The initial reaction conditions are defined by the electronic states of isolated H and Li_2 that are shown on the left-hand side of each reaction. These initial conditions lead unambiguously to HLi_2 potential curves that have the C_{2v} symmetry labels shown in the center of each reaction. If H is inserted into the center of the Li_2 bond, LiHLi linear molecules are obtained which have the $D_{\infty h}$ symmetry labels given on the right-hand side of each reaction. In the case of two curves that have the same symmetry, X is used to denote the lowest curve and A is used to denote the upper curve. For example, X^2A_1 (eq 1) refers to the lowest energy curve of $^2A_1$ symmetry and A^2A_1 (eq 3) refers to the next highest energy curve of $^2A_1$ symmetry.

Collinear Dissociation of LiHLi. Collinear dissociation reactions will be characterized by the potential energy curves and orbital contours for the $C_{\infty v}$ symmetry departure of Li from LiHLi shown on Figure 1b. There is a reactive cone about the LiLi′ axis for reactions of Li′ with the H^- end of LiH.[1,3] Since this cone includes the collinear path drawn on Figure 1b, an analysis of the corresponding collinear path ab initio potential energy curves and orbital contours will hopefully provide a realistic description of Li_2H dissociation.

We shall discuss the four lowest energy ab initio potential energy curves. In this case the curves provide static ab initio descriptions of the collinear reactions

$$LiHLi(^2\Sigma_g^+) \rightarrow LiHLi(A^2\Sigma^+) \rightarrow LiH(^1\Sigma^+) + Li(^2P) \quad (5)$$

$$LiHLi(^2\Sigma_u^+) \rightarrow LiHLi(X^2\Sigma^+) \rightarrow LiH(^1\Sigma^+) + Li(^2S) \quad (6)$$

$$LiHLi(^2\Pi_u) \rightarrow LiHLi(X^2\Pi) \rightarrow LiH(^1\Sigma^+) + Li(^2P) \quad (7)$$

$$LiHLi(^2\Pi_g) \rightarrow LiHLi(A^2\Pi) \rightarrow LiH(^3\Pi) + Li(^2S) \quad (8)[20]$$

Each initial reaction condition on the left-hand side is the same as the corresponding final label shown on the right-hand side of eq 1-4. This correlates HLi_2 formation and dissociation as was done in our original paper.[2]

Note that the accessible pathways lead to either ground state products (eq 6) or products containing excited Li atoms (eq

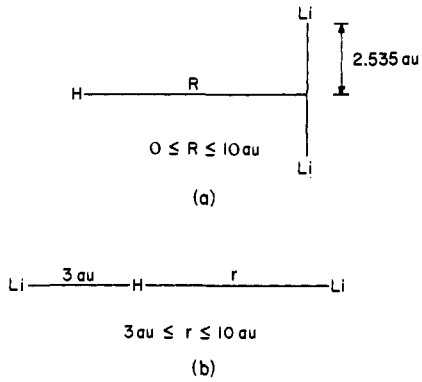

Figure 1. Li_2H geometries: (a) broadside; (b) collinear.

5 and 7). The excited state product of eq 8, $LiH(^3\Pi)$, is only slightly bound and probably dissociates by mixing with the repulsive $^3\Sigma^+$ state along C_s symmetry paths.

Results and Discussion

Overall Character of Li_2H ab Initio Potential Energy Curves. The character of the ab initio potential energy curves for the Li_2H molecule is summarized in Figure 2. Figure 2a describes the crossing of ionic and covalent single configuration molecular orbital (MO) curves of the same symmetry. The wave function for the upper curve usually does not satisfy the variational theorem. Covalent and ionic mixing is not observed in single configuration MO wave functions and charge transfer is abrupt.[11,13] Figure 2b is the potential curve which results when only the lower energy MO curve is drawn and emphasizes the abrupt charge transfer. There are two points to be made concerning the MO energy curves. As we shall discuss below, this abrupt charge transfer is not in general manifest in more accurate wave functions. For this reason MO's must be used cautiously for the discussion of reactions, as is well known. It is frequently impossible to calculate MO energies for excited states which have the same symmetry as lower energy states. Consequently, we shall use the natural orbitals of correlated MC-CI wave functions to obtain the ab initio interpretation of Li_2H reactions. This interpretation will also be phrased in the less accurate, but more familiar, MO language. In this way we emphasize the general ability of natural orbitals to characterize reaction intermediates and the fact that a qualitative MO interpretation can generally only be given after the natural orbitals have been determined. In this context, we hope to show under what circumstances such approximate MO interpretations can be judged reliable.

Figure 2c describes the interaction of ionic and covalent multiconfiguration (MC-CI) potential energy curves of the same symmetry. Both lower and upper curve wave functions satisfy the variational theorem. Covalent and ionic mixing can occur and the curves no longer cross. In this case the charge transfer is gradual. Figure 2d is the potential curve that results when only the lower energy curve of Figure 2c is drawn.

It is apparent from Figure 2 that the covalent Li_2H states lie below the ionic Li_2H states only when the atom-diatom pair is weakly interacting. As the interaction increases the covalent states become more repulsive and the ionic states become more attractive: This ultimately leads to ionic bound states. All of the lowest lying bound states of Li_2H are ionic in character.

We shall superimpose ab initio potential energy curves like those shown schematically on Figures 2b and 2d with orbital contours and occupation numbers in subsequent sections. This simultaneously presents the potential energy curves and the electronic charge distributions. Each potential curve and each set of orbital contours and occupation numbers corresponds to one of the reactions described in eq 1-8.

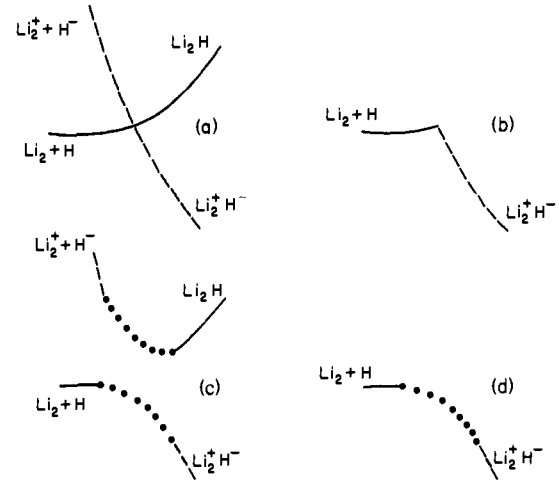

Figure 2. Schematic overall character of Li_2H ab initio potential energy curves. Increasing energy is plotted vertically upward for each case. The horizontal axis is the distance from H to the midpoint of the Li_2 bond as H approaches on a broadside or C_{2v} symmetry path. The $Li_2 + H$, $Li_2^+ + H^-$ asymptotes correspond to the left-hand part of each figure. Molecular states of Li_2H correspond to the right-hand part of each figure. The solid curves refer to covalent character. The dashed lines refer to ionic character. The dotted lines refer to mixtures of ionic and covalent character. (a) Crossing of single configuration curves. (b) Abrupt change in character of the lower energy molecular orbital curve due to the crossing. (c) Interaction of correlated potential energy curves. (d) Gradual change in character in the lower correlated energy curve due to the interaction.

Orbitals and Orbital Contours. Two types of orbitals were computed in our previous Li_2H work,[2,3] MO's and MC orbitals. In this work we computed approximate natural orbitals (NO's) for the MC wave functions using Löwdin's formalism.[9] The NO's are an orthogonal transformation of the MC orbitals and hence leave the total multiconfiguration-configuration interaction (MC-CI) energy invariant.[2] (This is true because all possible excitations of the three valence electrons within the truncated orbital space are included in the MC-CI wave function.) The NO's generally provide a compact description since the first-order density becomes a sum of intraorbital contributions. Only two or three NO's are needed to characterize the states in Li_2H. These points can be appreciated by considering the first-order density matrix for the lowest state of $^2B_2$ symmetry at $R = 5$ au. The expansion of the density matrix in terms of the MC orbitals is given as

$$\rho(1) = (\text{core}) + 1.26175\cdot 1s(1)^2 + 0.99970\cdot 2\sigma_u(1)^2 + 0.73645\cdot 2\sigma_g(1)^2 + 0.59070\cdot 1s(1)\cdot 2\sigma_g(1) + 0.02975\cdot 1s(1)\cdot 1\pi_u(1) - 0.03096\cdot 2\sigma_g(1)\cdot 1\pi_u(1) - 0.00883\cdot 2\sigma_u(1)\cdot 1\pi_g(1) + 0.00179\cdot 1\pi_u(1)^2 + 0.00030\cdot 1\pi_g(1)^2$$

in terms of the orbital labels we define below. In contrast, the NO expansion of the density is

$$\rho(1) = (\text{core}) + 1.64662\cdot 1s(1)^2 + 0.99978\cdot 2\sigma_u(1)^2 + 0.35291\cdot 2\sigma_g(1)^2 + 0.00046\cdot 1\pi_u(1)^2 + 0.00022\cdot 1\pi_g(1)^2$$

The core term refers to the doubly occupied Li 1s orbitals and is the same in both expansions. The cross terms in the expansion of $\rho(1)$ in the MC orbital basis cannot be simply interpreted. The diagonal bilinear NO expansion, however, is equivalent to a classical distribution function, and the electrons appear, on the average, to occupy the natural orbitals without regard to correlation effects involving more than one NO.[14] Similar statements apply to any observable which is a function of $\rho(1)$ only.[14]

The orbital contours were drawn with the plotting program developed by the Iowa State University-Ames Laboratory

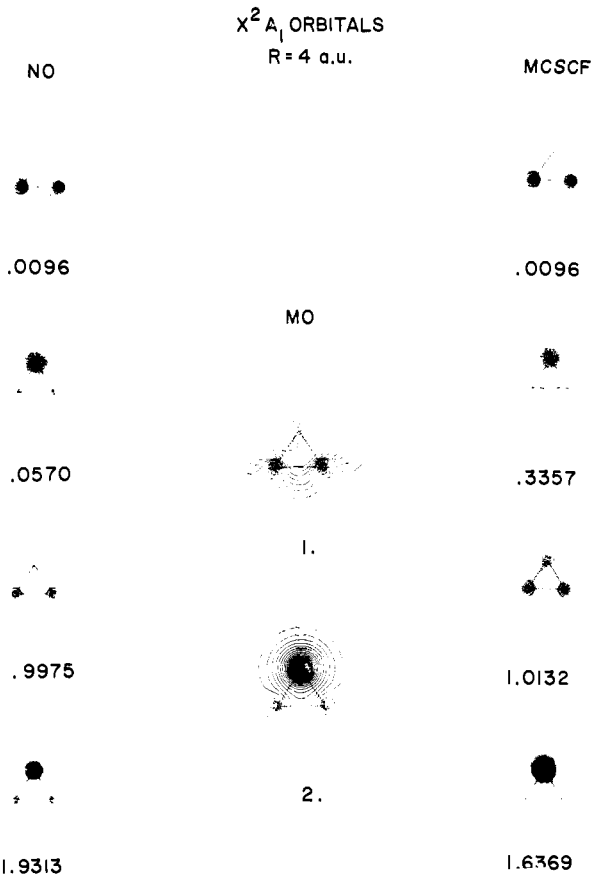

Figure 3. Comparison of NO's, MO's, and MC orbitals.

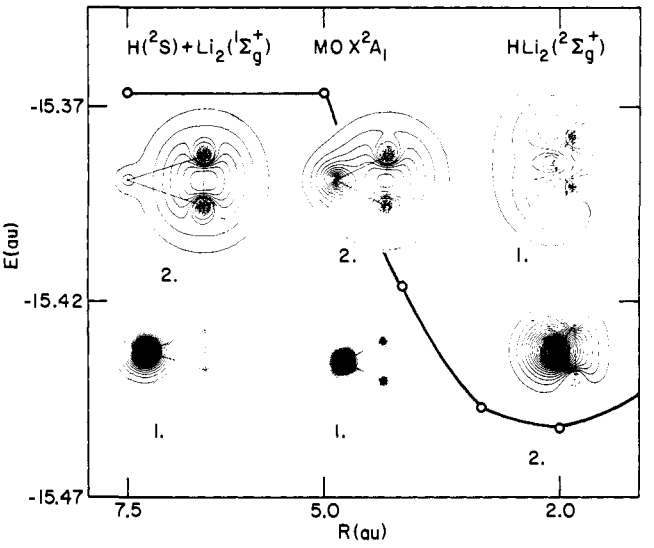

Figure 4. MO's for $H + Li_2 \rightarrow HLi_2$.

Theoretical Chemistry Group.[15] Contours for the C_{2v} formation path were projected onto the plane defined by the three atoms. Contours for the $C_{\infty v}$ dissociation path were projected onto a plane containing the linear Li-H-Li axis. The program calculates the orbital maxima, minima, and nodes and then plots successive contours according to an input increment (0.03 $au^{-3/2}$ in this case). Positive contours are drawn as solid lines, negative contours are drawn with dashed lines, and nodes are drawn as dotted lines. Only principal NO's are plotted.

A comparison of NO's, MO's, and MC orbitals is given on Figure 3 for the X^2A_1 wave functions at $R = 4$ au (see Figure 1). The MC orbitals are drawn under the column MC-SCF. The hydrogens are placed at the uppermost vertices of the triangles formed by the bond skeletons. Occupation numbers[9] are shown for the NO's and MO's. The analogous quantities for the MC orbitals are the diagonal elements of the first-order density matrix, and these are also included in the figure. The shapes and occupations of the NO's and MO's are similar. This is not true in general, even when the electronic wave function is approximately a single configuration. The reason is that when curve crossings are involved the single dominant configuration in the correlated wave function frequently differs from the single configuration MO wave function. In this case the NO description is not expected to resemble the MO description. We shall elaborate below. The NO and MO shapes and occupations clearly differ from those of the MC orbitals. The interpretation of the NO and MO description is a doubly occupied 1s on H, i.e., H^-, and a singly occupied orbital derived from $2\sigma_g$ on Li_2, i.e., Li_2^+. The MC description cannot be readily interpreted. This is typical of the present MC orbitals and is not surprising since the purpose of the MC calculations was to provide orbitals for use in the subsequent configuration interaction calculations.[2] Consequently we cannot use the MC orbitals for interpretive purposes. The bottom row orbitals are all largely centered on H. The MC orbital has a much smaller negative contribution on Li_2 than do the NO and MO orbitals. This shows that orthogonality requirements with respect to the Li_2 inner shells are not solely responsible for the negative contributions on Li_2 which are observed in the NO and MO H^- type orbitals, i.e., the negative contributions in the NO and MO H^- orbitals represent physical interactions.

Genealogical Orbital Labels. This section describes a labeling method that was used for the ab initio wave functions and orbital contours. It is based on the observation that a given orbital's genealogy can usually be traced by viewing its contours. For example, the 1s orbital on H can be easily recognized in both Li_2H and LiH. Therefore, instead of using labels which apply to the molecules, e.g., the 2σ orbital in the case of LiH, the orbital will always be labeled 1s. The occupation of the 1s is almost always nearly one or nearly two. In the latter cases it will sometimes be referred to as an H^- 1s orbital to emphasize the charge transfer. The other labels we shall use are $2\sigma_g$, $2\sigma_u$, $1\pi_u$, and $1\pi_g$, which are taken from Li_2; σ and π, which refer to σ symmetry and π symmetry "lone pairs" on LiH; and 2s and 2p, which are taken from Li. The Li inner shells are constant throughout and are not explicitly labeled.

This labeling scheme simplifies the notation without increasing the likelihood of confusion. It should be kept in mind that orbitals may show common characteristics, e.g., contributions from 1s will be apparent in $2\sigma_g$ and vice versa. However, the dominant character can always be unambiguously established from the orbital contours.

$H(^2S) + Li_2(^1\Sigma_g^+) \rightarrow HLi_2(X^2A_1) \rightarrow HLi_2(^2\Sigma_g^+)$. The MO and NO potential energy curves and orbital contours for X^2A_1 are drawn in Figures 4 and 5, respectively. Proceeding from left to right across the top of the figures, the labels describe the initial states of the separated $H + Li_2$ systems (^2S and $^1\Sigma_g^+$), the electronic state of the C_{2v} symmetry Li_2H molecule (X^2A_1), and the electronic state of the linear $D_{\infty h}$ LiHLi molecule ($^2\Sigma_g^+$). The hydrogen is always the left-hand vertex of the triangular bond skeleton. The contours are drawn for $R = 7.5$, 5, and 2 au (see Figure 1), proceeding from left to right across the figures. Occupation numbers are given for each set of contours. This basic format will be followed for the rest of the figures in the paper.

The MO contours and occupations in Figure 4 describe abrupt charge transfer from the covalent MO configuration $1s2\sigma_g^2$ to the ionic MO configuration $1s^2\sigma_g$, i.e., $H^-Li_2^+$. The charge transfer occurs when the covalent and ionic potential energy curves cross near $R = 5$ au.

The NO contours and occupations on Figure 5 describe the

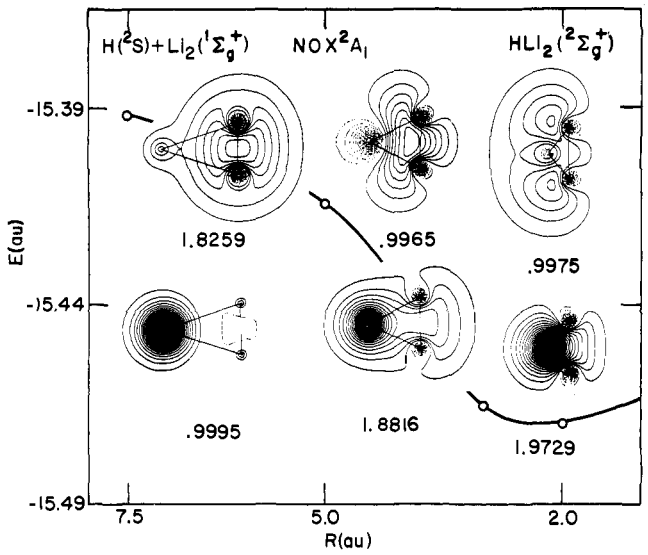

Figure 5. NO's for $H + Li_2 \rightarrow HLi_2$.

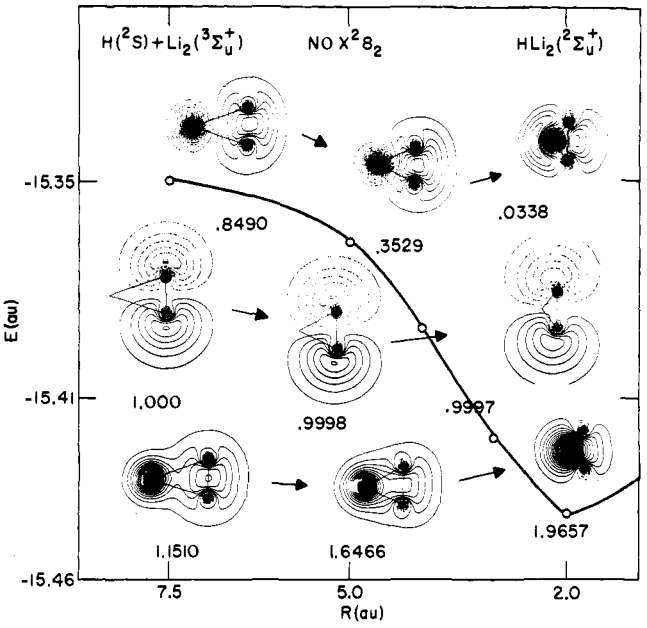

Figure 6. NO's for $H + Li_2^* \rightarrow HLi_2^*$.

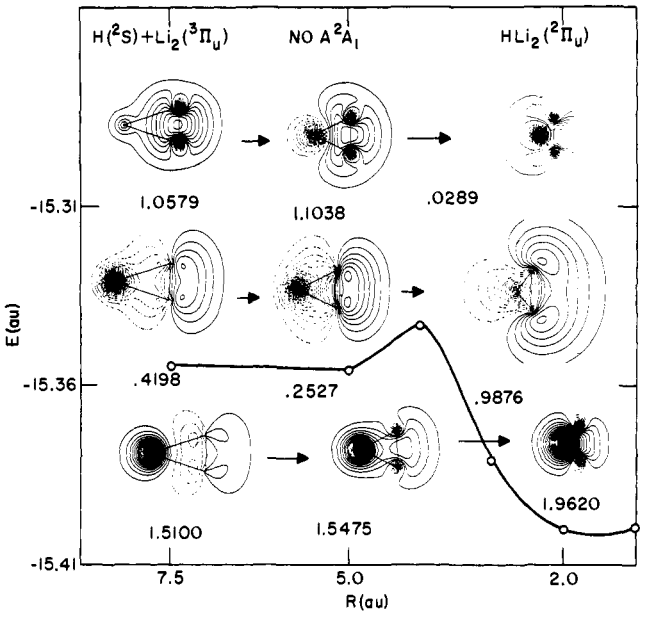

Figure 7. NO's for $H + Li_2^{**} \rightarrow HLi_2^{**}$.

gradual transfer of one electron from the $2\sigma_g$ NO to the 1s NO. Note that this gradual process achieves charge transfer at larger R values than would be predicted from the MO results in Figure 4. The MO and NO occupations and contours at R = 5 au are different: charge transfer has occurred in the NO description, but not in the MO description. The MO and NO occupations at R = 4 au (see Figure 3) are approximately the same: charge transfer has taken place in both descriptions.

The upper row NO and MO orbitals at R = 7.5 au closely resemble the $2\sigma_g$ orbitals in isolated Li_2. The major characteristics of the $2\sigma_g$ orbital are negative contributions at the Li nuclei and positive contours which are most concentrated in the bond region, but which surround the whole molecule. This bears directly on the negative contours which appear in the 1s orbitals following the charge transfer process. Note that the H^- NO at R = 2 shows substantially more negative contours around the Li_2 nuclei than does the corresponding MO. The interpretation is that the charge transfer NO has assumed more of the characteristics of the covalent $2\sigma_g$ orbital than has the charge transfer MO. This is interesting in that the doubly occupied MO shown in Figure 3 also assumes $2\sigma_g$ covalent character that is comparable to the corresponding 1s NO. Thus the covalent character of the 1s NO's is maintained as R decreases, but the covalent character of the 1s MO's varies qualitatively as R decreases. Similar remarks apply to the $2\sigma_g$ orbitals. Following charge transfer, negative contours appear around H in the $2\sigma_g$ NO's. Although the number of contours involved decreases, the negative contours surrounding H are maintained as R decreases. Figure 4 shows that in the case of the MO's the negative contours have all but vanished at R = 2 au.

It is natural to wonder if the difference between the NO's and the MO's is related to the well-known nonuniqueness of the MO's.[16] This is apparently not the case, the reason being that here the different valence MO's are in general occupied differently. In the case mentioned in the preceding paragraph, one valence MO is always singly occupied and the other is always double occupied. Therefore, orthogonal transformations of the valence MO's do not leave the total energy invariant, i.e., the valence MO's are unique.

$H(^2S) + Li_2(^3\Sigma_u^+) \rightarrow HLi_2(X^2B_2) \rightarrow HLi_2(^2\Sigma_u^+)$. NO contours for these potential surface cuts are shown in Figure 6. The interpretation provided is that the upper $2\sigma_g$ NO gradually transfers its electron to the lower 1s NO as R decreases. Note that the sum of the two fractional occupation numbers equals 2 at all R. Note also that during the transfer the 1s assumes $2\sigma_g$ character and vice versa. Upon completion of the charge transfer, the 1s NO closely resembles the corresponding NO in Figure 5, while the $2\sigma_g$ orbital becomes a correlating orbital.

The NO interpretation is gradual charge transfer from the 3 open-shell configuration $1s2\sigma_u2\sigma_g$ to the ionic configuration $1s^22\sigma_u$ via the mechanism just described. The MO interpretation can be deduced from Figure 3 of ref 2. Abrupt charge transfer occurs near R = 4 au where the ionic $1s^22\sigma_u$ and covalent $1s2\sigma_u2\sigma_g$ curves cross.

$H(^2S) + Li_2(^3\Pi_u) \rightarrow HLi_2(A^2A_1) \rightarrow HLI_2(^2\Pi_u)$. Figure 7 shows NO contours for the first excited state of $^2A_1$ symmetry. For $R \gg 7.5$ au, the configuration must be $1s2\sigma_g1\pi_u$ since this is the second lowest energy configuration of $Li_2 + H$ that has A_1 symmetry. The R = 7.5 au contours show that $1\pi_u$ begins to gradually transfer its electron to 1s. The sum of the nonintegral $1\pi_u$ and 1s NO occupation numbers is approximately 2; the 1s NO clearly assumes some of the character of the $1\pi_u$

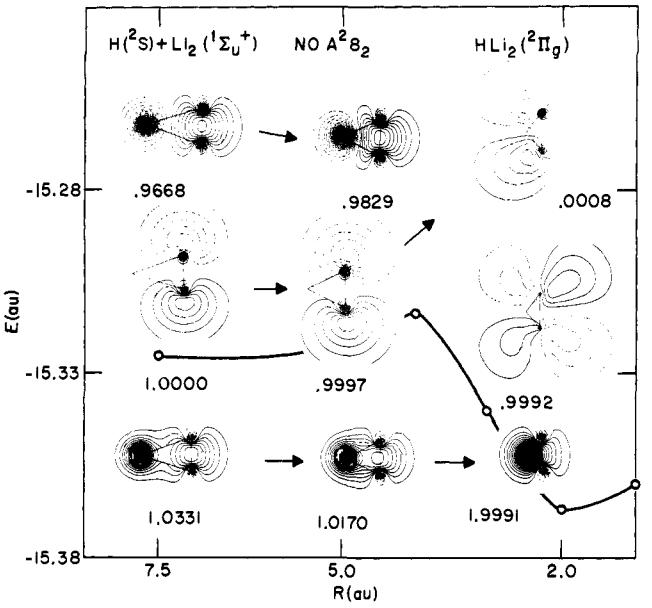

Figure 8. NO's for H + Li_2*** → HLi_2***.

NO and vice versa. Thus the charge transfer in Figure 7 begins much like the charge transfer recorded in Figure 6. However, the NO contours at $R = 5$ au do not show a continuation of the $1\pi_u \rightarrow 1s$ charge transfer. This is consistent because continuation of the $1\pi_u \rightarrow 1s$ charge transfer yields the ionic configuration $1s^2 2\sigma_g$, which is the dominant X^2A_1 charge transfer configuration and therefore cannot also dominate A^2A_1. The configurations $1s2\sigma_g 1\pi_u$, $1s^2 2\sigma_g$, and $1s2\sigma_g^2$ have mixing coefficients in the MC wave function which are equal to 0.4342 (1s and $2\sigma_g$ coupled to triplet spin), 0.3151 (1s and $2\sigma_g$ coupled to singlet spin), 0.3360, and 0.7271, respectively at $R = 5$ au. If each configuration were simply given an equal weight, an NO occupancy of $1s^{1.3} 2\sigma_g^{1.3} 1\pi_u^{0.3}$ would result. Since the actual occupancy shown in Figure 7 at $R = 5$ au is $1s^{1.5475} 2\sigma_g^{1.1038} 1\pi_u^{0.2527}$, this shows qualitatively how the fractional NO occupancies arise.

The NO contours at $R = 2$ au correspond to the charge transfer configuration $1s^2 1\pi_u$. The $1\sigma_g$ NO transfers its occupation to 1s and $1\pi_u$. This charge transfer is more abrupt than the previous cases shown in Figures 5 and 6. Note that the curve in Figure 7 shows a hump at $R = 4$ au. This hump is not a barrier in a dynamically significant sense. Lower energy C_{2v} symmetry paths corresponding to slightly longer Li-Li bonds are not expected to show such humps.

The MO representation of the A^2A_1 curve involves three curve crossings. The covalent $1s2\sigma_g 1\pi_u$ and ionic $1s^2\sigma_g$ MO curves cross near $R = 6$ au. Next, the ionic $1s^2 2\sigma_g$ and covalent $1s2\sigma_g^2$ curves cross near $R = 4$ au. Finally, the covalent $1s2\sigma_g^2$ and ionic $1s^2 1\pi_u$ curves cross near $R = 3$ au. The last crossing involves configurations which differ by a two-electron replacement. Only the last curve crossing can be discerned from the NO analysis; the first two crossings become so gradual that they are not recognizable.

$H(^2S) + Li_2(^1\Sigma_u^+) \rightarrow HLi_2(A^2B_2) \rightarrow HLi_2(^2\Pi_g)$. Figure 8 shows the NO representation of the excited state A^2B_2 potential energy curve. The charge transfer process is straightforward: the $2\sigma_g$ and $2\sigma_u$ NO's each transfer an electron to the $1\pi_g$ and 1s NO's near $R = 4$ au. The charge transfer is abrupt An interesting feature is the appearance of the $1\pi_g$ NO and the corresponding disappearance of the $2\sigma_g$ and $2\sigma_u$ NO's. The remnants of the $2\sigma_u$ NO at $R = 2$ au are shown at the top right of the figure as is indicated by the arrows. It is clear from both the contours and the occupation number that at $R = 2$ au the $2\sigma_u$ NO is a correlating orbital. Note how its contours adapt to the presence of the $1\pi_g$ NO. Finally, the hump at $R = 4$ au in Figure 8 is not dynamically significant for the same reasons as were given in connection with Figure 7.

The MO description of the charge transfer is that the covalent $1s2\sigma_g 2\sigma_u$ MO energy curve crosses the ionic $1s^2 1\pi_g$ curve near $R = 4$ au. This curve crossing involves MO configurations which differ by two-electron replacements. On the basis of this and the preceding sections, it appears that when the MO representation of the charge transfer involves curve crossings whose MO configurations differ by two-electron replacements, abrupt charge transfer also occurs in the NO representation. In the present cases, the two-electron charge transfer processes correspond to interactions between single configurations which differ by two occupied orbitals. The configuration mixings are then proportional to two-electron interactions in lowest order, and the dominant configuration can be expected to change abruptly, much as in an actual curve crossing.

$LiHLi(^2\Sigma_g^+) \rightarrow LiHLi(A^2\Sigma^+) \rightarrow LiH^-(^2\Sigma^+) + Li^+(^1S)$. The NO contours shown in Figure 9 correspond to the collinear dissociation of LiHLi shown in Figure 1b. From left to right across the top of Figure 9, the labels describe the electronic state of the $D_{\infty h}$ symmetry linear molecule ($^2\Sigma_g^+$), the electronic state of the $C_{\infty v}$ linear molecule ($A^2\Sigma^+$), and the electronic states of two sets of dissociation asymptotes which can be recognized in the LiH···Li molecule ($LiH^-(^2\Sigma^+) + Li^+(^1S)$ and $LiH(^1\Sigma^+) + Li(^2P)$). The contours drawn correspond to $r = 3$, 4, 7.5, and 10 au from left to right across the figure. In each set the Li in LiH is the left nucleus, the departing Li is the right nucleus, and H lies between them. The horizontal lines describe the linear bond skeletons. All other quantities are the same as in the C_{2v} contour plots. This format will be used for all collinear plots.

The arrows in Figure 9 are used to trace the evolution of a given NO. We connect the $A^2\Sigma^+$ curve to the $^2\Sigma_g^+$ state rather than to the almost degenerate $^2\Sigma_u^+$ state.[2] Our reasoning is that the contour plots for the singly occupied NO in Figure 9 show positive contours outside both Li nuclei as $r \rightarrow 3$ au, and this is consistent with a $^2\Sigma_g^+$ connection. The contours shown below the filled circle on the potential curve are the MO's obtained at $r = 10$ au. These MO's closely resemble the atom-diatom NO's for $LiH(X^1\Sigma^+) + Li^*(^2P)$. Since we did not compute the asymptotic NO's in this work, we have used the MO's and indicated this by the dashed portion of the energy curve.

The doubly occupied NO at the left of the figure is the H^- like NO which was encountered in the discussion of Li_2H formation. At the right of the figure it is the H^- like orbital in LiH. The MO's shown at the far right demonstrate that the doubly occupied orbital need not have significant negative contributions around the Li in LiH. That is, orthogonality constraints alone do not require that the H^- orbital show significant negative contours around the Li in LiH. However, the H^- NO's consistently show such negative contours. This can be interpreted as a covalent feature of the ionic LiH bond, and in particular as an antibonding feature. Similar but more pronounced negative contours occur in both the NO and MO descriptions of the perfectly covalent $Li_2(X^1\Sigma_g^+)$ bond. In the case of Li_2, however, the negative contours are everywhere surrounded by the positive contours of the covalent bond, i.e., the effect of the negative contours in Li_2 is not of simple antibonding.

As the Li begins to withdraw from LiH, the odd electron goes into a σ lone pair on the Li side of LiH. This is reasonable because of the ionic structure of LiH, Li^+H^-. We initially found the potential curve in Figure 9 to be quite puzzling. Contour diagram analysis identified the intermediate species as Li^+···LiH^-. Theoretical calculations[17,18] predict that the

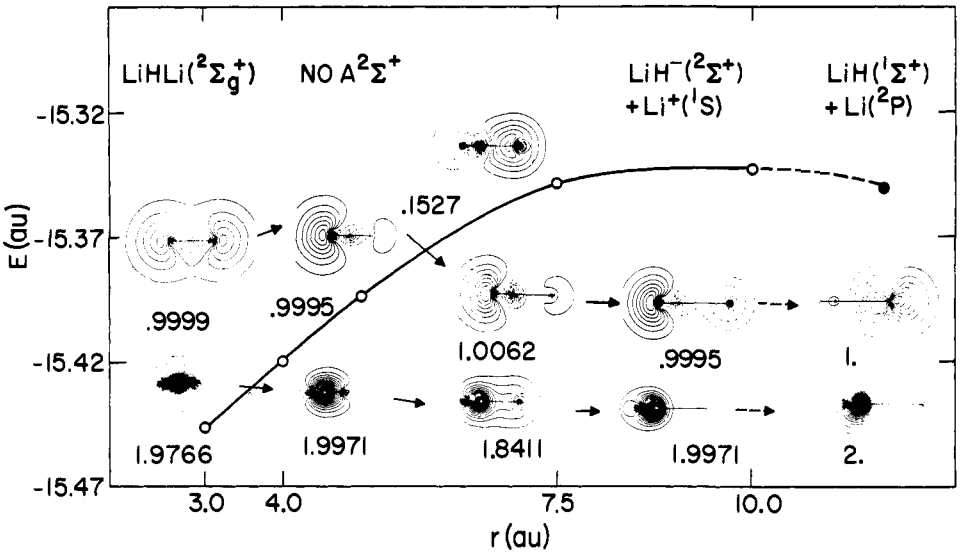

Figure 9. NO's for LiHLi → LiH$^-$···Li$^+$ → LiH + Li*.

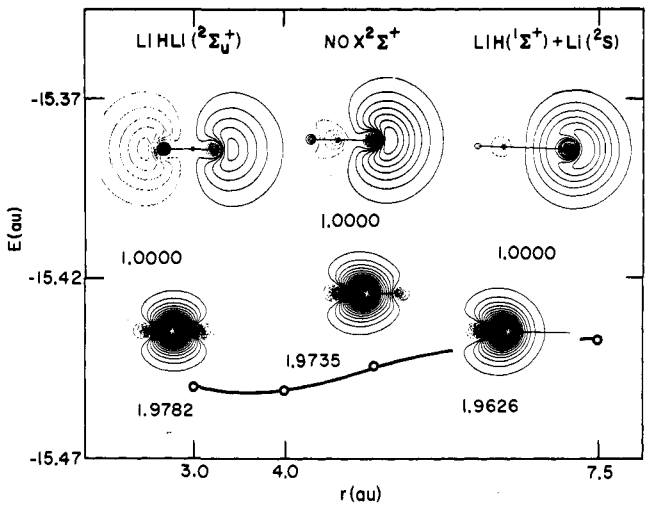

Figure 10. NO's for LiHLi* → LiH + Li.

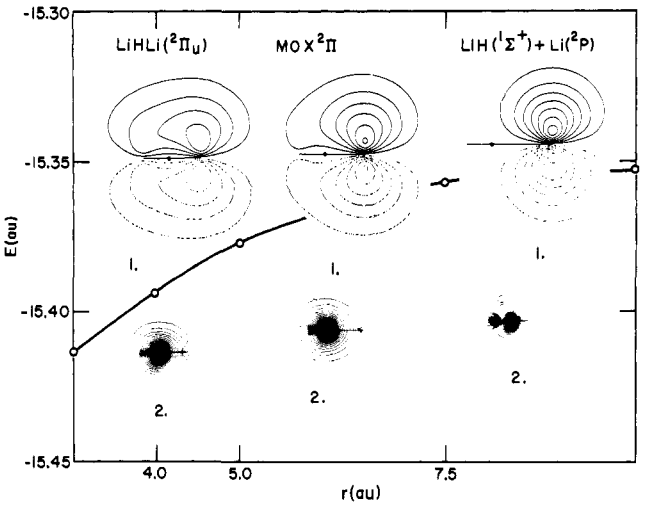

Figure 11. MO's for LiHLi** → LiH + Li*.

electron affinity of LiH is about 0.3 eV, so the Li$^+$···LiH$^-$ intermediate appears quite reasonable.

The potential curve becomes slowly varying around r = 7.5 au and there is interaction with a 2s NO on the departing Li. This corresponds to the gradual charge transfer and fractional occupation numbers encountered in Figure 6. In the present case the transfer process involved is $1s^2 \rightarrow 1s2s$, which would produce the open-shell configuration $1s\sigma2s$, where σ is the singly occupied "lone pair" on LiH (or the 3σ orbital in LiH). However, the interaction with 2s has disappeared at r = 10 au and the σ "lone pair" is beginning to move onto the departing Li. The ultimate charge transfer will thus be $\sigma \rightarrow 2p$ to give the configuration $1s^22p$, as is shown by the MO's beneath the filled circle in Figure 9. The MC-CI wave functions do contain the necessary configurations to describe this charge transfer process. We did not, however, extend our curves to the larger r values where the charge transfer occurs.

The MO representation of the $A^2\Sigma^+$ curve probably consists of two curve crossings as r increases. The first crossing corresponds to $1s^2\sigma \rightarrow 1s\sigma2s$ and probably occurs near r = 7.5 au. The second curve crossing corresponds to $1s\sigma2s \rightarrow 1s^22p$ and probably occurs before r = 10 au. Note that this last crossing involves two orbital changes. Closer estimates for either crossing are unavailable because the excited state MO calculations could not actually be carried out in most cases.

LiHLi($^2\Sigma_u^+$) → LiHLi($X^2\Sigma^+$) → LiH($^1\Sigma^+$) + Li(^{2}S). The NO contours that describe the formation of ground state products are shown in Figure 10. The plots were made at r = 3, 4, and 7.5 au. The contours describe straightforward dissociation of LiHLi to ground state LiH and Li. The NO description is the same as is obtained with MO's, which can be anticipated by the integral occupation numbers and the absence of charge transfer.

LiHLi($^2\Pi_u$) → LiHLi($X^2\Pi$) → LiH($^1\Sigma^+$) + Li(^{2}P). MC-CI wave functions were not computed for this process. The MO's for the collinear dissociation are shown in Figure 11. The contours are drawn at r = 4, 5, and 7.5 au. Dissociation proceeds as in Figure 10, except that here one asymptote is Li(^{2}P). The MO description is probably very similar to what would be obtained with NO's since no charge transfer or other curve crossings are involved.

LiHLi($^2\Pi_g$) → LiHLi($A^2\Pi$) → LiH$^-$($^2\Pi$) + Li$^+$(^{1}S). MC-CI energy curves were not computed for this process. In the MO approximation the $A^2\Pi$ state of LiHLi dissociates along collinear paths to the ion pair LiH$^-$($^2\Pi$) + Li$^+$(^{1}S). This is shown in Figure 12. The MO's are drawn at r = 4, 5, 7.5, and 10 au.

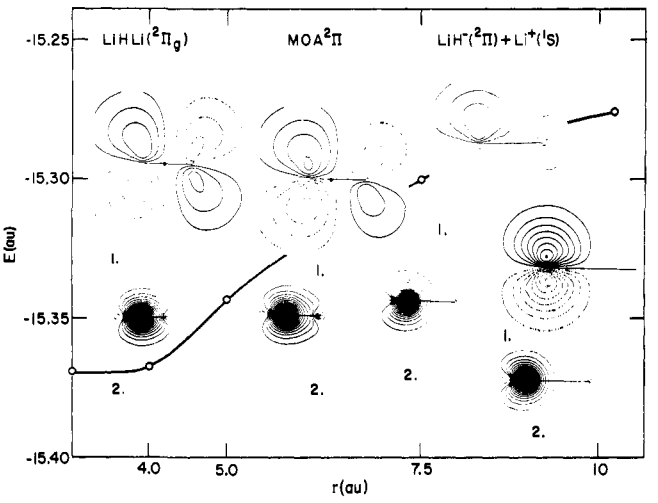

Figure 12. MO's for LiHLi*** → LiH⁻ + Li⁺.

The evolution of the ion pair is a gradual process proceeding from small to large r values. There is already noticeable ionic character at $r = 5$ au. According to Figure 2 of ref 2, the ionic $LiH^-(2\Pi)\cdots Li^+(^1S)$ curve will cross $^2\Pi$ symmetry covalent curves near $r = 7.5$ au. The covalent curves describe the open-shell configurations $1s\pi 2s$, where π is a singly occupied π "lone pair" on LiH that corresponds to a LiH 1π orbital.[19] Hence, the MO prediction for $A^2\Pi$ is abrupt charge transfer from LiH^- to Li^+ near $r = 7.5$ au, followed by dissociation to $LiH(^{1,3}\Pi) + Li(^2S)$. (See, however, the remark for eq 8.) It is again worth pointing out that the LiH^-, Li^+ intermediates were not identified until after the orbital contours were analyzed.

The NO description of $A^2\Pi$ is probably not like the NO description of $A^2\Sigma^+$ shown in Figure 10. In the present case the net charge transfer is $1s^2 \rightarrow 1s2s$, and the π "lone pair" remains singly occupied when $r \rightarrow \infty$. Since there are no other curves of Π symmetry in this energy range, the charge transfer is probably accomplished like the case shown in Figure 6. That is, we expect fractional occupation numbers and gradual charge transfer from $1s^2$ to 1s2s. This will be manifest by the energy curve shown in Figure 12 becoming a slowly varying function of r beyond $r \approx 7.5$ au.

Conclusions

Analysis of MO and NO orbital contour plots and occupation numbers for the low-lying electronic states of Li^2H has identified the chemical structures of the intermediate species involved. The NO and MO descriptions of the ionic $Li_2^+H^-$ bound states agree with one another. However, NO and MO descriptions of the atom-diatom pairs $Li_2 + H$ and $LiH + Li$ generally are not the same. The reason for the disagreement is that the NO's usually show charge transfer to be a gradual process whereas MO's show charge transfer to be an abrupt process. Consequently, the correlated wave functions display ionic character to noticeably larger atom-diatom separations than do the uncorrelated MO wave functions. Hence, MO's should not be used to interpret the details of charge transfer, even for ground state to ground state reactions. In the case of excited states which have the same symmetry as lower energy states, the MO's usually cannot be calculated.

The NO results interpret reactions 1-4 in the following overall ways

$$H(1s) + Li_2(2\sigma_g^2) \rightarrow H^-(1s^2)Li_2^+(2\sigma_g) \quad (1')$$

$$H(1s) + Li_2^*(2\sigma_g 2\sigma_u) \rightarrow H^-(1s^2)Li_2^{+*}(2\sigma_u) \quad (2')$$

$$H(1s) + Li_2^{**}(2\sigma_g 1\pi_u) \rightarrow H^-(1s^2)Li_2^{+} {}^{**}(1\pi_u) \quad (3')$$

$$H(1s) + Li_2^{***}(2\sigma_g 2\sigma_u) \rightarrow H^-(1s^2)Li_2^{+} {}^{***}(1\pi_g) \quad (4')$$

where the asterisks refer to excited states. It is found that "one-electron, one-orbital" transfers such as occur in eq 1′ occur gradually, i.e., over larger ranges of $H + Li_2$ separations. On the other hand, it is found that "two-electron, two-orbital" transfers such as appear in eq 4′ occur more abruptly, i.e., over smaller ranges of $H + Li_2$ separations. Equation 3′ involves more than one type of transfer. The first two are one-electron, one-orbital processes, roughly speaking $1s1\sigma_g 1\pi_u \rightarrow 1s^2 2\sigma_g$, followed by $1s^2 2\sigma_g \rightarrow 1s2\sigma_g^2$. The latter transfer is required because $1s^2 2\sigma_g$ becomes the dominant NO representation of ground state $H^-Li_2^+$. The final transfer is basically $1s2\sigma_g^2 \rightarrow 1s^2 1\pi_u$ and is rather abrupt. Because of this complicated process, the NO's have fractional occupation numbers.

The overall NO interpretation of reactions 5 and 6 are

$$H^-(1s^2)Li_2^+(2\sigma_g) \rightarrow Li(\sigma)H^-(1s^2)\cdots Li^+ \quad (5')$$

$$\rightarrow Li^+H^-(1s^2) + Li^*(2p) \quad (5'')$$

$$H^-(1s^2)Li_2^+(2\sigma_u) \rightarrow Li^+H^-(1s^2) + Li(2s) \quad (6')$$

where σ is a singly occupied σ symmetry lone pair on Li in LiH. In keeping with one-electron, one-orbital transfers, the charge transfer from the right side of eq 5′ to eq 5″ products is accomplished gradually.

NO descriptions of reactions 7 and 8 were not computed in this work. Based on the results found for eq 5 and 6, the predicted NO descriptions are

$$H^-(1s^2)Li_2^+(1\pi_u) \rightarrow Li^+H^-(1s^2) + Li(2p) \quad (7')$$

$$H^-(1s^2)Li_2^+(1\pi_g) \rightarrow Li(\pi)H^-(1s^2)\cdots Li^+ \quad (8')$$

$$\rightarrow LiH(1s\pi)^{**} + Li(2s) \quad (8'')[20]$$

where π is a singly occupied π symmetry lone pair on Li in LiH.

MO contours were plotted for eq 7′ and 8′. Equation 7′ is a case where the MO and NO descriptions are expected to be very similar, so the MO's themselves provide an accurate representation. The MO's for eq 8′ clearly showed the charge transfer and the π orbital. It can therefore be predicted that the NO's will correspond to gradual charge transfer from the right side of eq 8′ to eq 8″.

Acknowledgments. We are grateful to M. Dombek, K. Sundberg, and K. Ruedenberg of the Iowa State University-Ames Laboratory Theoretical Chemistry Group for kindly providing the contour plotting program. N.H.S. thanks Dr. P. Fortune of Argonne for helpful discussions. We are also grateful to Dr. A. Wagner of Argonne for his reading of the manuscript and for several useful suggestions. This work was performed under the auspices of the Division of Physical Research of the U.S. Energy Research and Development Administration.

References and Notes

(1) P. Siegbahn and H. F. Schaefer, III, *J. Chem. Phys.*, **62**, 3488 (1975).
(2) W. B. England, N. H. Sabelli, and A. C. Wahl, *J. Chem. Phys.*, **63**, 4596 (1975).
(3) W. B. England, N. H. Sabelli, A. C. Wahl, and A. Karo, *J. Phys. Chem.*, **81**, 772 (1977).
(4) A. L. Companion, *J. Chem. Phys.*, **48**, 1186 (1968).
(5) J. C. Tully, *J. Chem. Phys.*, **58**, 1396 (1973).
(6) C. H. Wu and H. R. Ihle, *J. Chem. Phys.*, **66**, 4356 (1977).
(7) W. Stwalley, private communication.
(8) L. Pauling and E. B. Wilson, Jr., "Introduction to Quantum Mechanics", McGraw-Hill, New York, N.Y., 1935.
(9) P. O. Löwdin, *Phys. Rev.*, **97**, 1474 (1955).
(10) Y. T. Lee, R. J. Gordon, and D. R. Herschbach, *J. Chem. Phys.*, **54**, 2410 (1971).
(11) J. L. Magee, *J. Chem. Phys.*, **8**, 667 (1940).
(12) D. M. Linsay, D. R. Herschbach, and A. L. Kwiram, *Mol. Phys.*, **32**, 1199 (1976).
(13) F. T. Smith, *Phys. Rev.*, **179**, 111 (1969).

(14) J. M. Ziman, "Elements of Advanced Quantum Theory", Cambridge University Press, Cambridge, 1969, p 97.
(15) M. Dombek, K. R. Sundberg, and K. Ruedenberg, private communication.
(16) W. England, L. S. Salmon, and K. Ruedenberg, *Fortshr. Chem. Forsch.*, **23**, 31 (1971), and references therein.
(17) K. D. Jordan, K. M. Griffing, J. Kenney, E. L. Andersen, and J. Simons, *J. Chem. Phys.*, **64**, 4730 (1976).
(18) B. Liu, K. O.-Ohata, and K. Kirby-Docken, *J. Chem. Phys.*, **67**, 1850 (1977).
(19) C. F. Melius and W. A. Goddard, III, *J. Chem. Phys.*, **56**, 3348 (1972).
(20) Deviations from the linear symmetry in this case will give the products Li(^{2}S) + H(^{2}S) + Li(^{2}S) since the in-plane component of $^3\Pi$ mixes with the repulsive $^3\Sigma^+$ surface as $^2A'$ along C_s symmetry paths.

Theoretical Analysis of Long-Range Hyperfine Interactions in Bicyclic Free Radicals. Application Conditions for the W and Anti-W Rules

Y. Ellinger,*†[1a] R. Subra,‡[1a] and G. Berthier†[1b]

Contribution from Laboratoire de Chimie Organique Physique, Département de Recherche Fondamentale, C.E.A.-C.E.N. Grenoble, 85 X, F. 38041 Grenoble Cedex, France, and Laboratoire de Chimie Quantique, F. 75005 Paris, France.
Received December 12, 1977

Abstract: The ab initio spin-restricted SCF and perturbative configuration interaction methods have been applied to the bicyclobutyl radical. Long-range interactions are found to be critically dependent on the geometry at the radical site. The conditions required for a correct assignment of long-range couplings by means of the W rule are presented. As in aliphatic radicals, strong couplings come from a cumulative effect of the spin-delocalization and spin-polarization contributions.

Long-range interactions have aroused considerable interest because of their high stereospecificity and unusual values, especially in bicyclic radicals.[2] Assignment of the observed couplings is made in most cases following the so-called "W arrangement".[2a] However, the conditions required for applying the W rule are still a matter of discussion.

In this respect, we wish to report the main results of an ab initio study of proton hyperfine couplings in the simplest bicyclic radical, i.e., the bicyclobutyl radical observed by Krusic et al. some years ago.[3] Our main goal has been to investigate how long-range interactions can be modified by structural deformations occurring at the radical site. The geometrical parameter which has been varied is the torsion angle α between the CH bond and the CCC plane. All other parameters have been kept constant and taken from bicyclobutane.[4] No geometry optimization has been attempted.[5]

The ground-state wave function is calculated according to the two Hamiltonian spin-restricted SCF formalism developed by Roothaan.[6] A configuration interaction including all spin-adapted monoexcited configurations with three uncoupled electrons is then carried out using the Epstein-Nesbet formulation of perturbation theory.[7] The total Fermi contact splitting of any nucleus M is given by

$$a_M = a_d + a_{sp}$$

where

$$a_d = \left(\frac{8\pi}{3}\right)\left(\frac{g_e}{g_0}\right) g_M \beta_M |\phi_u(r_M)|^2$$

$$a_{sp} = \left(\frac{8\pi}{3}\right)\left(\frac{g_e}{g_0}\right) g_M \beta_M \sum_d \sum_{v^*} -2\frac{\langle \phi_u \phi_d | \phi_u \phi_{v^*} \rangle}{E_0 - E_{d\to v^*}} \phi_d(r_M)\phi_{v^*}(r_M)$$

The ϕ_d are the doubly occupied MOs of the ground state, the ϕ_{v^*} are the virtual MOs, and ϕ_u is the orbital containing the unpaired electron. Under those conditions a_d and a_{sp} correspond to the contributions arising from the delocalization effects (at the SCF level) and from the spin-polarization effects (at the CI level), respectively.[8] For coherence with our preceding studies of hydrocarbon radicals,[9] the same Gaussian basis (9s,5p/4s) has been used and the canonical MOs have been converted into quasi-localized MOs according to the same localization criterion.[10]

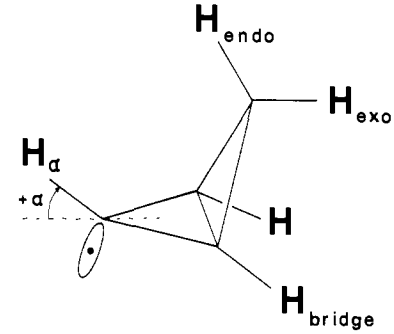

The variation of proton hyperfine splittings with torsion at the radical site is presented in Figure 1. All couplings are given in gauss. Tables I and II present numerical tabulations of H_{endo} and H_{exo} coupling constants as functions of α.

α and β Coupling Constants. The present calculations confirm the high sensitivity of the α hydrogen coupling with bending at the radical site. The negative coupling found for $\alpha = 0°$ which is almost entirely due to the spin polarization becomes positive for $|\alpha| > 30°$ as a consequence of the rapid increase of the delocalization contribution.

For the β hydrogens (H bridge), the point to be outlined is that the coupling constant decreases when the H_α is moved toward the exo direction ($\alpha < 0$) more rapidly than when it is moved toward the endo direction ($\alpha < 0$). As a consequence, for a given torsion of the radical center, the coupling constant of a β proton trans with respect to the orbital containing the unpaired electron should be lower than the coupling constant of a cis proton.

Experimental examples of inequivalent couplings are known for β protons in bicyclic radicals deriving from the bicy-

† Centre National de la Recherche Scientifique (E.R.A. no 20 et L.A. no. 77).
‡ Université Scientifique et Médicale de Grenoble (E.R.A. no. 20).

0002-7863/78/1500-4961$01.00/0